Draft version January 7, 2021
Typeset using LaTeX **twocolumn** style in AASTeX63

Dynamics of Colombo's Top: Tidal Dissipation and Resonance Capture

Yubo Su[1] and Dong Lai[1]

[1] *Cornell Center for Astrophysics and Planetary Science, Department of Astronomy, Cornell University, Ithaca, NY 14853, USA*

(Received XXXX; Revised XXXX; Accepted XXXX)

Submitted to ApJ

ABSTRACT

Abstract here

Keywords: planet—star interactions

1. INTRODUCTION

- Studying planetary obliquities is important. Cassini States are key.
- In CS, resonance when two frequencies g and $\alpha\cos\theta$ become commensurate, $g \simeq \alpha\cos\theta$, where θ is the planetary obliquity.
- Many works consider entry into a CS by having g or α vary over time to effect resonance capture (e.g. Anderson & Lai 2018; Millholland & Batygin 2019; Su & Lai 2020; Anderson & Lai 2020). However, a third possibility exists: θ can evolve and sweep through a resonance, e.g. under tidal friction.
- Resonance capture via separatrix crossing was first considered by (Henrard 1982) for non-dissipative perturbations (e.g. Su & Lai 2020). However, tidal friction is dissipative, so this formalism does not apply. We show that this generalizes.

2. THEORY AND EQUATIONS

In this section, we first briefly lay out the spin dynamics of the planet, introducing the Cassini State spin-orbit resonance (for more details, see Su & Lai 2020). We then introduce the equilibrium tide model of weak tidal friction used in this work (Lai 2012). While there are many models of tidal dissipation that may be more accurate (e.g. CITE), our qualitative conclusions do not depend on the specific model used, so we use the equilibrium tide model for simplicity.

Corresponding author: Yubo Su
yubosu@astro.cornell.edu

2.1. *Spin Dynamics Without Tidal Friction*

We consider a star of mass $M_\star$ hosting an inner oblate planet of mass m and radius R with semi-major axis a and an outer planet of mass m_p with semi-major axis a_p and eccentricity e_p. Let the inner planet be spinning with spin $\mathbf{s}$ (with $s \equiv |\mathbf{s}|$ the spin angular velocity and $\hat{\mathbf{s}}$ the spin orientation), and call the unit angular momenta of the inner and outer planets' orbits $\hat{\mathbf{l}}$ and $\hat{\mathbf{l}}_\mathrm{p}$ respectively. The equations of motion in the absence of tidal friction are:

$$\frac{\mathrm{d}\hat{\mathbf{s}}}{\mathrm{d}t} = \omega_\mathrm{sl}\left(\hat{\mathbf{s}}\cdot\hat{\mathbf{l}}\right)\left(\hat{\mathbf{s}}\times\hat{\mathbf{l}}\right) - \omega_\mathrm{lp}\cos I\left(\hat{\mathbf{s}}\times\hat{\mathbf{l}}_\mathrm{p}\right), \tag{1}$$

$$\omega_\mathrm{sl} \equiv \frac{3GJ_2mR^2M_\star}{2a^3I\Omega} = \frac{3k_q}{2k}\frac{M_\star}{m}\left(\frac{R}{a}\right)^3 s, \tag{2}$$

$$\omega_\mathrm{lp} = \frac{3m_p}{4M_\star}\left(\frac{a}{a_\mathrm{p}\sqrt{1-e_\mathrm{p}^2}}\right)^3 n. \tag{3}$$

In Eq. (2), $I = kmR^2$ (with k a constant) is the moment of inertia and $J_2 = k_\mathrm{q}s^2(R^3/Gm)$ (with k_q a constant) the rotation-induced (dimensionless) quadrupole of the planet [for a body with uniform density, $k = 0.4, k_q = 0.5$; for rocky planets, $k \simeq 0.2$ and $k_{qp} \simeq 0.17$ (e.g. Lainey 2016) ? not sure]. In other studies, $3k_\mathrm{qp}/2k_\mathrm{p}$ is often notated as $k_2/2C$ (e.g. Millholland & Batygin 2019). In Eq. (3), $n \equiv \sqrt{GM_\star/a^3}$ is the inner planet's orbital mean motion, and we have assumed $a_\mathrm{p} \gg a$ and included only the leading-order (quadrupole) interaction between the planet and disk. Following standard notation, we define $\alpha = \omega_\mathrm{sl}$ and $g \equiv -\omega_\mathrm{1p}\cos I$ (e.g. Colombo 1966).

We define s_c to be the critical spin where

$$\alpha|_{s=s_\mathrm{c}} = -g. \tag{4}$$

2.2. *Cassini States*

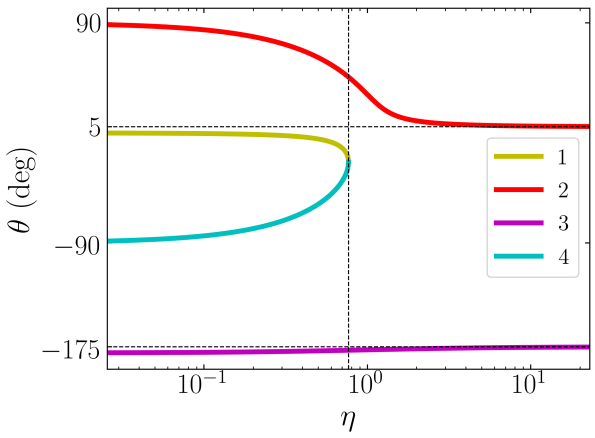

Figure 1. CS locations, TODO change axis labels etc.

Equilibria of spin dynamics are *Cassini States* (CSs). Refer to Su & Lai 2020 for more detailed discussion. In the notation of the previous paper,

$$\eta \equiv -\frac{g}{\alpha} = \frac{s_c}{s}. \tag{5}$$

Plots of CS locations as always in Fig. 1.

Note that ϕ is conjugate to $\cos\theta$, and thus the spin dynamics obey Hamiltonian:

$$H(\mu,\phi;s) = -\frac{s}{s_c}\frac{\mu^2}{2} + \mu\cos I - \sin I\sqrt{1-\mu^2}\cos\phi. \tag{6}$$

Plot of level curves of Hamiltonian as before, including $C_\pm$ notation in Fig. 2.

2.3. *Weak Tidal Friction*

We implement the weak friction theory of equilibrium tides (Lai 2012), under which both θ and s evolve. We define the dimensionless time

$$\tau \equiv gt. \tag{7}$$

The full equations of motion including weak tidal friction are then

$$\frac{d\hat{\mathbf{s}}}{d\tau} = \frac{s}{s_c}\left(\hat{\mathbf{s}}\cdot\hat{\mathbf{l}}\right)\left(\hat{\mathbf{s}}\times\hat{\mathbf{l}}\right) - \hat{\mathbf{s}}\times\hat{\mathbf{l}}_p + \frac{\epsilon 2n}{s}\left(1 - \frac{s}{2n}\left(\hat{\mathbf{l}}\cdot\hat{\mathbf{s}}\right)\right)\hat{\mathbf{s}}\times\left(\hat{\mathbf{l}}\times\hat{\mathbf{s}}\right), \tag{8}$$

$$\frac{ds}{d\tau} = \epsilon 2n\left(\hat{\mathbf{s}}\cdot\hat{\mathbf{l}} - \frac{s}{2n}\left(1 + \left(\hat{\mathbf{s}}\cdot\hat{\mathbf{l}}\right)^2\right)\right), \tag{9}$$

where ϵ measures the tidal dissipation rate and is given by

$$\epsilon \equiv -\frac{1}{gt_a}\frac{L}{2S}\frac{s}{2n}, \tag{10}$$

$$\frac{1}{t_a} = \frac{3k_2}{Q}\left(\frac{m}{M}\right)\left(\frac{R}{a}\right)^5 n. \tag{11}$$

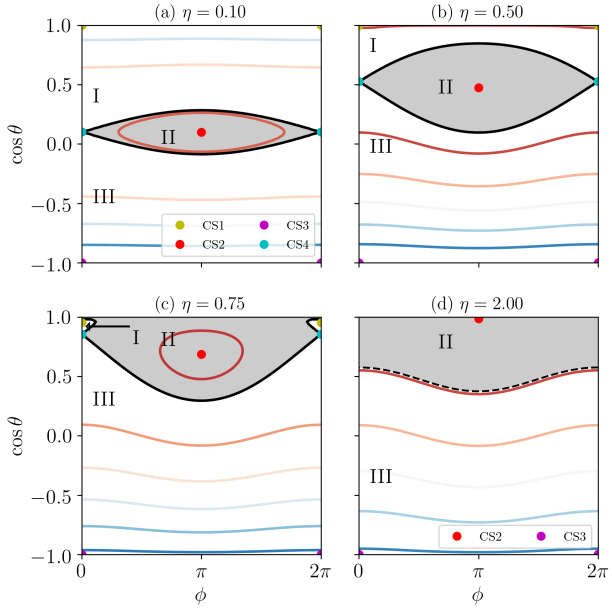

Figure 2. TODO label $C_\pm$.

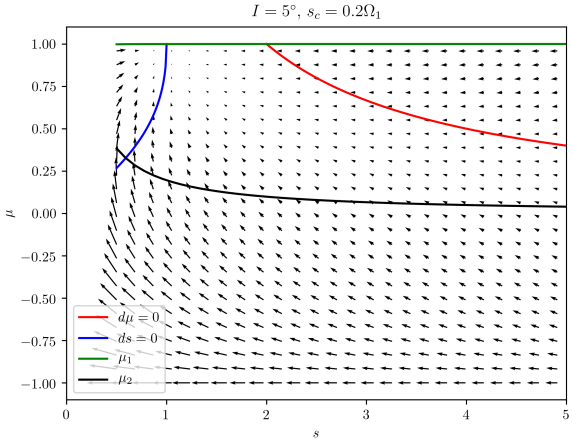

Figure 3. Phase portrait.

Here, L and S are the orbital and spin angular momenta of the inner planet, respectively.

The phase portrait for these EOM in (s,θ) space is shown in Fig. 3. Note that the semimajor axis a is not constant, but $\dot{a}/\dot{\theta} \sim S/L \ll 1$, and is negligible for our problem (but not always, Millholland tidal runaway cite).

2.4. *Stable Equilibria of Tidal Friction*

Generally, these EOM have equilibria at the points that are both a CS and satisfy $\dot{s} = 0$ under weak tidal friction. These are stable when ignoring tidal friction (Su & Lai 2020). On Fig. 3, these are the intersection of the locations of CS1 and CS2 with the line $\dot{s} = 0$. It is clear that the locations of these

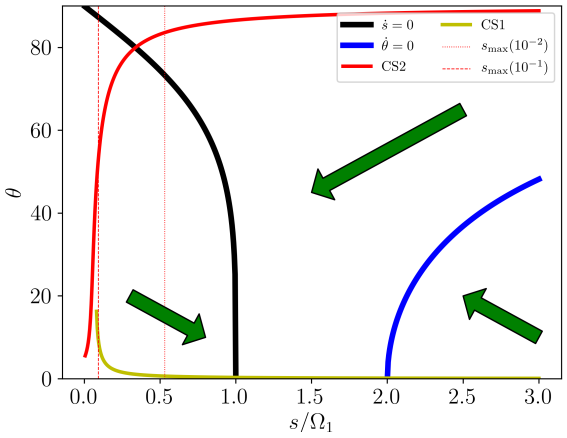

Figure 4. Location of tCE. Vertical line is spin rate below which tCE is destroyed.

equilibria depend on the value of s_c. Call these generalized equilibria *tidal Cassini Equilibria* (tCE), and number them tCE1 and tCE2 depending on whether they are CS1 or CS2 states. Shown

Furthermore, if tides are too strong (large ϵ), tCE2 can become unstable (cite Fabrycky). The required ϵ for stability of tCE2 is given by

$$\epsilon \leq \frac{\eta_2 \sin I}{1-\mu_2^2}, \tag{12}$$

where η_2 and μ_2 are evaluated at tCE2.

3. PROBABILITY DISTRIBUTION OF OUTCOMES

The general question of the dynamics is then as follows: given problem parameters (including s_c) and an initial planet spin and obliquity (s, θ), what are the possible outcomes and their associated probabilities? We study this first at fixed s_c as a function of θ in Section 3.1, then as a function of s_c for an isotropic initial spin $\hat{s}$ in Section 3.2.

3.1. *Distribution As a Function of θ*

As a result of Section 2.4, the tCE are the only possible final outcomes. We generate initial spin vectors $\hat{s}$ for isotropic initial distribution $(\cos\theta, \phi)$, and average over ϕ in histograms. This gives histograms in Figs. **??**

Similarly to Su & Lai (2020), these probabilities are the result of separatrix crossings. However, the calculation differs from Su & Lai (2020): since the perturbation is dissipative in phase space (i.e. it does not conserve phase space area), analysis following Henrard (1982) is not sufficient. A more general theory of separatrix crossing is still able to predict the outcome probabilities. Appendix A.2 gives a more thorough overview of separatrix crossing dynamics, but the key result is:

$$a^2 + b^2 = c^2. \tag{13}$$

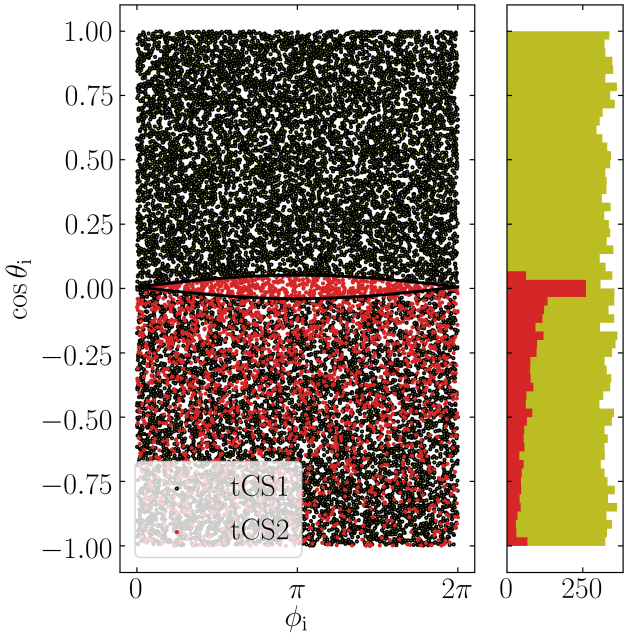

Figure 5. $s_c = 0.06$. Note that it is difficult to reach tCE2.

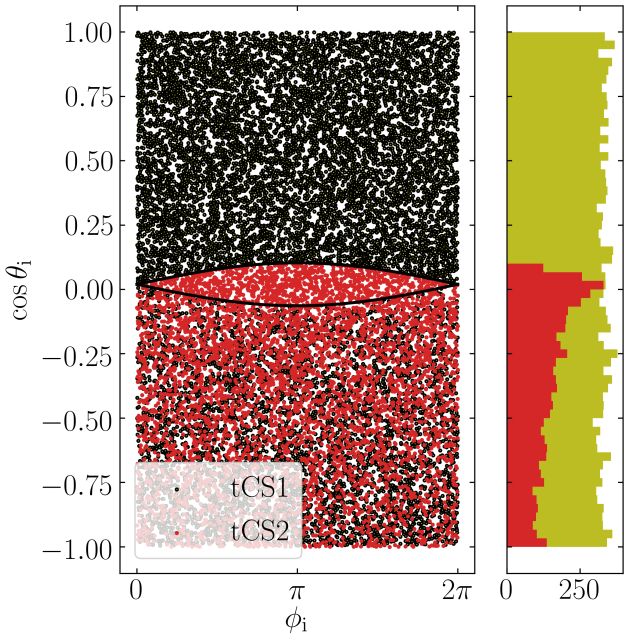

Figure 6. $s_c = 0.2$. Note that tCE2 is both reached with substantial probability and has substantial obliquity.

We can apply this curve to calculate the likelihood of the tCEs when a particular trajectory encounters the separatrix, and from this obtain a semi-analytical prediction of the distribution of outcomes. The semi-analytical nature of this calculation arises because $\eta_\star$ cannot be calculated *a priori*. The agreement of this curve with the histograms is examined for the same three s_c values in Figs. **??**.

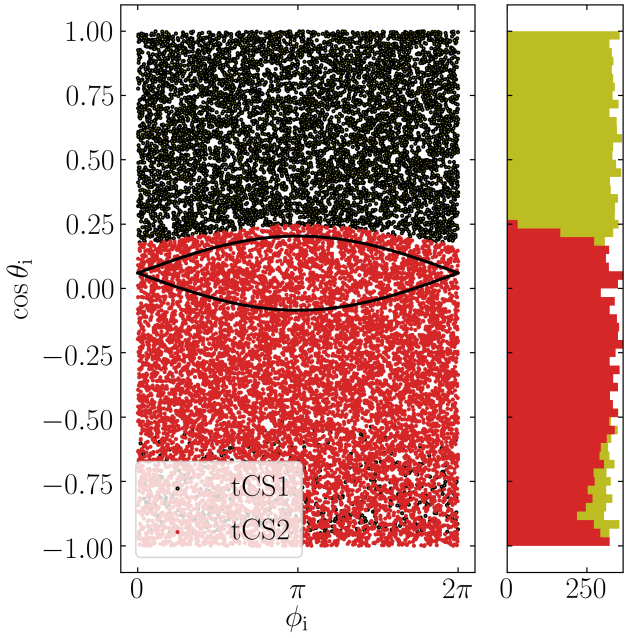

Figure 7. $s_c = 0.6$. Note that tCE2 becomes attracting over tCE1, but will have obliquity $\approx I$ and is uninteresting.

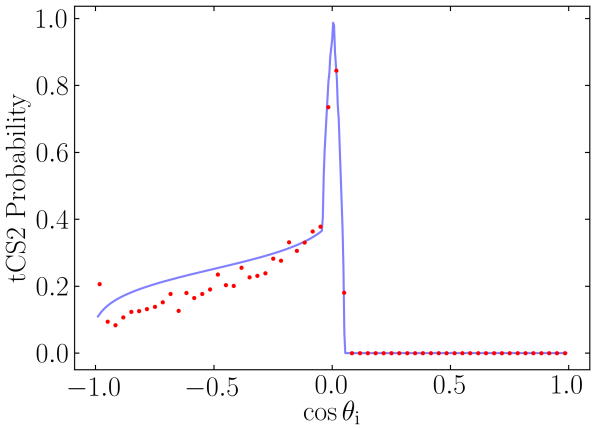

Figure 8. $s_c = 0.06$ prediction vs histogram.

3.2. *Distribution As a Function of s_c*

Assuming that $\hat{s}$ is drawn from an isotropic distribution, we may then calculate the probabilities of going to either tCE as a function of s_c. This is shown below for $I = 5°$

Note that while only the results for an isotropic distribution of initial $\hat{s}$ are shown, in principle arbitrary distributions $P(\theta_i)$ can be convolved against the $P_{tCE2}(\theta_i)$ distributions shown in Section 3.1.

4. SUMMARY AND DISCUSSION

REFERENCES

Anderson, K. R., & Lai, D. 2018, Monthly Notices of the Royal Astronomical Society, 480, 1402

—. 2020, The Astrophysical Journal, 906, 17

Colombo, G. 1966, SAO Special Report, 203

Henrard, J. 1982, Celestial Mechanics and Dynamical Astronomy, 27, 3

Lai, D. 2012, Monthly Notices of the Royal Astronomical Society, 423, 486

Lainey, V. 2016, Celestial Mechanics and Dynamical Astronomy, 126, 145

Millholland, S., & Batygin, K. 2019, The Astrophysical Journal, 876, 119

Su, Y., & Lai, D. 2020, arXiv preprint arXiv:2004.14380

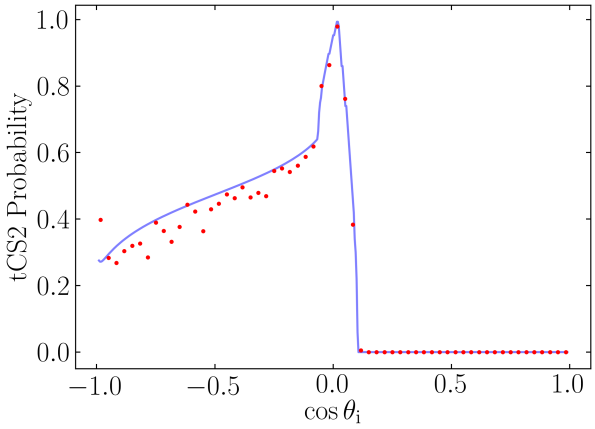

Figure 9. $s_c = 0.20$ prediction vs histogram.

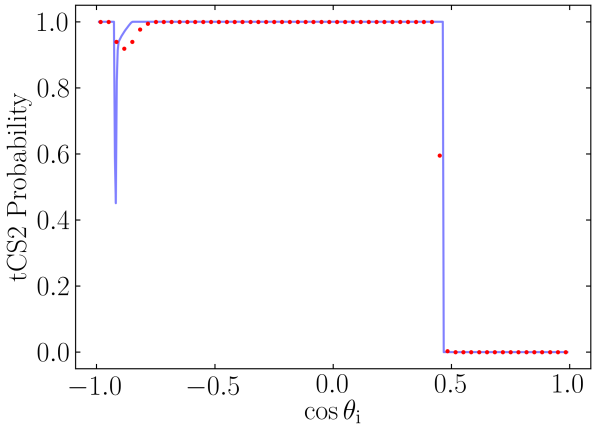

Figure 10. $s_c = 0.70$ prediction vs histogram.

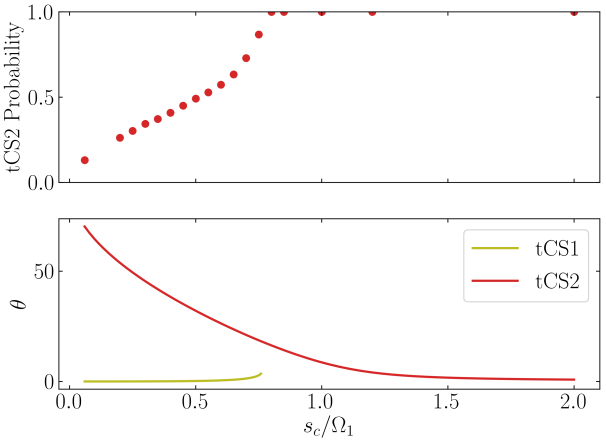

Figure 11. Top: total probability of ending up in tCE2 (blue dots) and the prediction ignoring separatrix capture (red line). Bottom: obliquities of the tCEs.

APPENDIX

A. SEPARATRIX CROSSING DYNAMICS

A.1. *Theory*

A.1.1. *Application of Adiabatic Invariance: Henrard Theory*

Review Henrard result, is already very successful e.g. MMR capture.

A.1.2. *Melnikov Integral*

The first substantial new result.

A.1.3. *Example: Constant s*

"Toy problem 1", the nice $P_c \propto \eta^{3/2}$ result. Application of Section A.1.2.

A.1.4. *Combined Result*

Thus, the natural extension of the two above results should be

$$\Delta_\pm = \oint_{C_\pm} \frac{\mathrm{d}H}{\mathrm{d}t}\,\mathrm{d}t, \tag{A1}$$

$$= \oint_{C_\pm} \dot{\mu}^{(1)} + \frac{\dot{s}^{(1)}}{\dot{\phi}^{(0)}}\left(\frac{\partial H}{\partial s} - \frac{\partial H_4}{\partial s}\right)\mathrm{d}\phi. \tag{A2}$$

A.2. *Separatrix Crossing Probability: Tidal Friction*

Application of the full formula presented in Section A.1. The key result is that one integrates

$$\frac{\mathrm{d}(\Delta H)}{\mathrm{d}(\epsilon t)} \approx (1-\mu^2)\left(\frac{2\Omega}{s} - \mu\right)\dot{\phi}^{(0)} + 2\Omega\left(1 + \frac{s}{2\Omega}(1+\mu^2)\right)\left[\frac{\mu^2}{2s_c} - \frac{s_c}{2s^2}\cos^2 I\right]. \tag{A3}$$

An analytical form that holds when $s \gg s_c$ is:

$$\begin{aligned}\frac{\Delta_\pm}{\epsilon} =& -2\cos I\left(\pm 2\pi\eta\cos I + 8\sqrt{\eta\sin I}\right) \pm 2\pi s\cos I + \eta\cos I\left(-8\sqrt{\sin I/\eta}\right) + \frac{s}{2}8\sqrt{\sin I/\eta} \\ &+ \frac{2\Omega}{s}\left(\mp 2\pi\left(1 - 2\eta\sin I\right) + 16\cos I\eta^{3/2}\sqrt{\sin I}\right) + 8\sqrt{\eta\sin I} \pm 2\pi\eta\cos I - \frac{64}{3}\left(\eta\sin I\right)^{3/2}.\end{aligned} \tag{A4}$$

The capture probability is then just

$$P_c = \frac{\Delta_+ + \Delta_-}{\Delta_-}. \tag{A5}$$